Supplementary information

Penetration of Nanobody-Dextran Polymer Conjugates through Tumor Spheroids

Peter Bitsch [1,†], Eva S. Baum [2,†], Irati Beltrán Hernández [2,3], Sebastian Bitsch [1], Jakob Harwood [1], Sabrina Oliveira [2,3,*], and Harald Kolmar [1,4,*]

[1] Institute for Organic Chemistry and Biochemistry, Technical University of Darmstadt, Peter-Grünberg-Str. 4, 64287 Darmstadt, Germany
[2] Cell Biology, Neurobiology and Biophysics, Department of Biology, Faculty of Science, Utrecht University, Padualaan 8, 3584 CH Utrecht, The Netherlands
[3] Pharmaceutics, Department of Pharmaceutical Sciences, Faculty of Science, Utrecht University, Universiteitsweg 99, 3584 CG Utrecht, The Netherlands
[4] Centre of Synthetic Biology, Technical University of Darmstadt.
* Correspondence: s.oliveira@uu.nl (S.O.); harald.kolmar@tu-darmstadt.de (H.K.)
† These authors contributed equally to this work.

Table of contents

1. Synthesis of compounds

1.1. Synthesis of cadaverine-azide linker

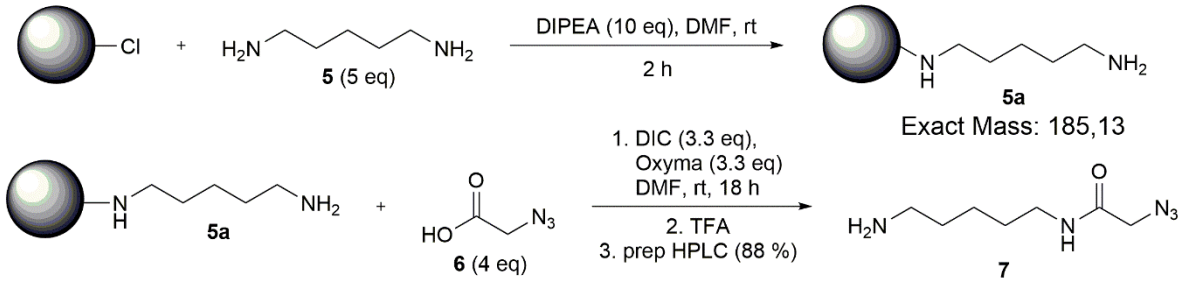

Scheme S 1. Synthesis of the N_3-Cad-Linker (*N*-(aminopentyl)-2-azidoacatamide).

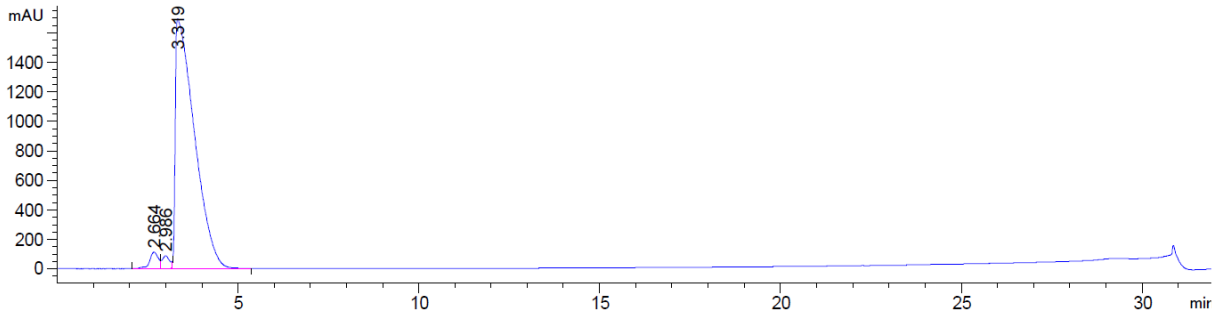

Figure S 1. HPLC-diagram of the N_3-Cad-Linker (0to80 % Eluent B, 220 nm).

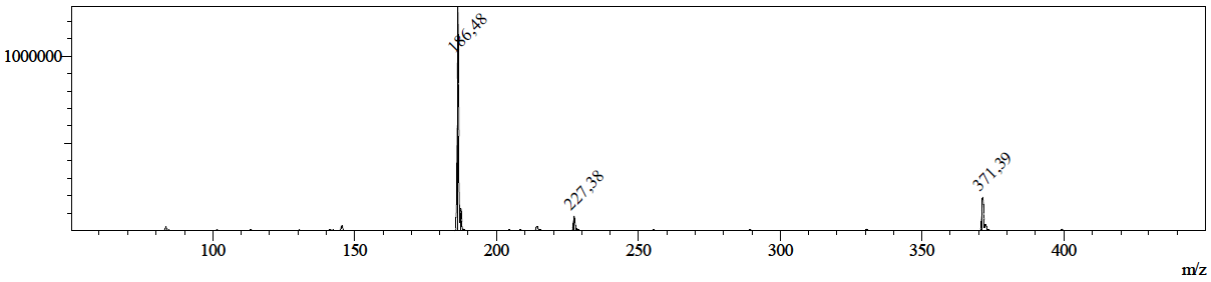

Figure S 2. LC-MS spectrum of the N_3-Cad-Linker (exact mass = 185.13 m/z). As method, a gradient from 10to100 % Eluent B was used over 20 min with a flow rate of 0.7 mL/s.

1.2. Synthesis of dextran-*N*-Boc-cadaverine

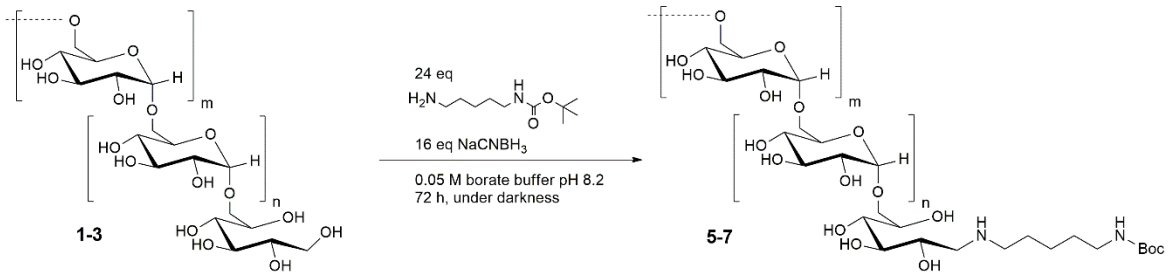

Scheme S 2. Reductive amination of dextran with *N*-Boc-cadaverine.

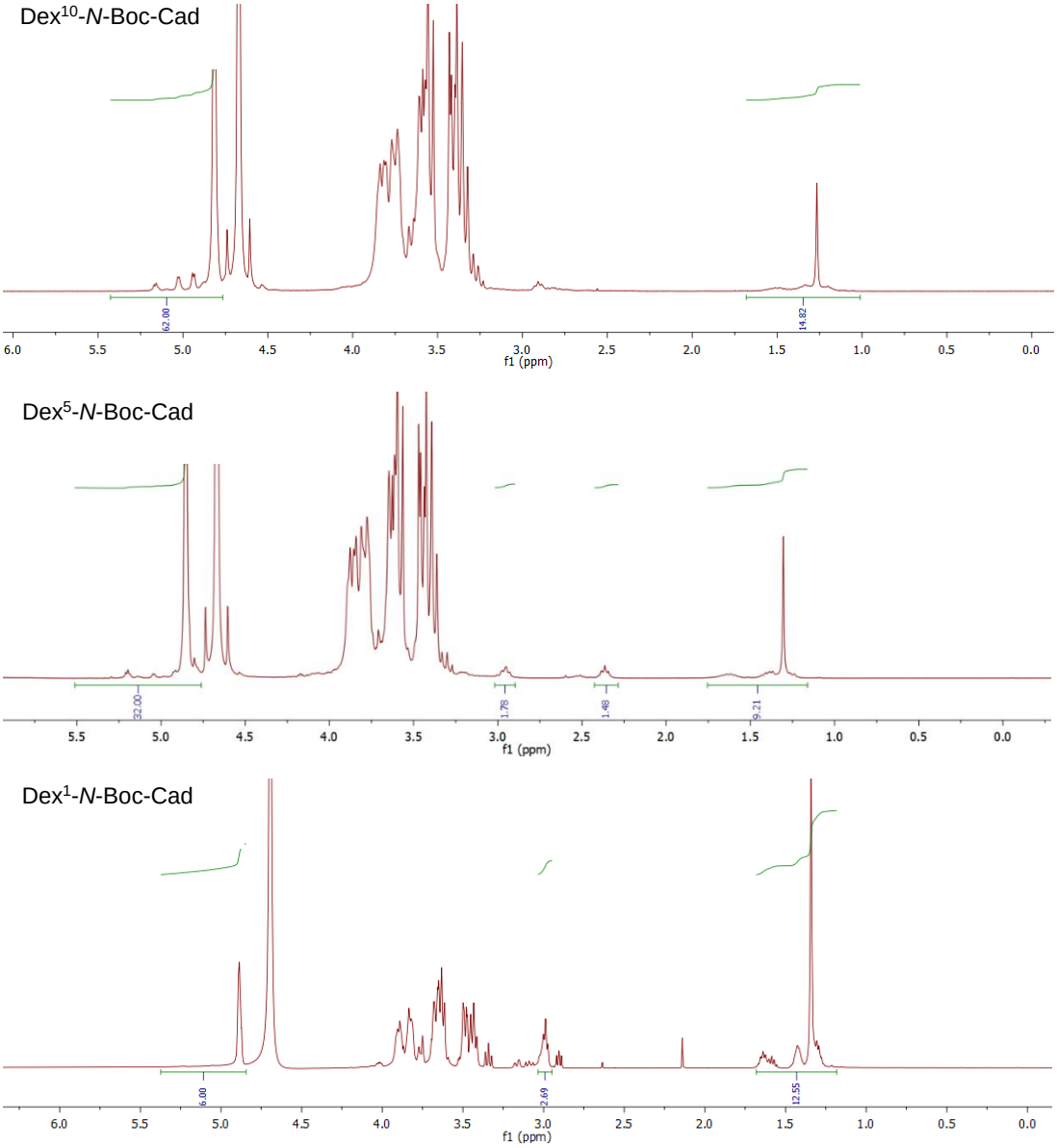

Figure S 3. ^{1}H-NMR spectra of Dex-*N*-Boc-Cad variants. ^{1}H-NMR (300 MHz, deuterium oxide) δ = 5.36 – 4.80 (m, 1 H, C(1)H), 4.20 – 3.22 (m, C(2-6)H (glucose units)), 3.05 – 2.81 (m, 4 H, C**H**$_2$NH-Boc, C**H**$_2$(CH$_2$)$_4$NHBoc), 1.73 – 1.19 (overlapped m, 15H, C**H**$_2$(CH$_2$)$_3$NH-Boc, C**H**$_2$(CH$_2$)$_2$NH-Boc, C**H**$_2$(CH$_2$)$_1$NH-Boc, 3 C**H**$_3$(Boc)) ppm.

1.3. Carboxyethylation of dextran

Table S 1. Calculated CE-ratios per dextran.

compound	CE-groups per dextran	Yield [%]
2-CED[10]-*N*-Boc-Cad	2.4	65
2-CED[5]-*N*-Boc-Cad	2.4	73
2-CED[1]-*N*-Boc-Cad	4.3	45

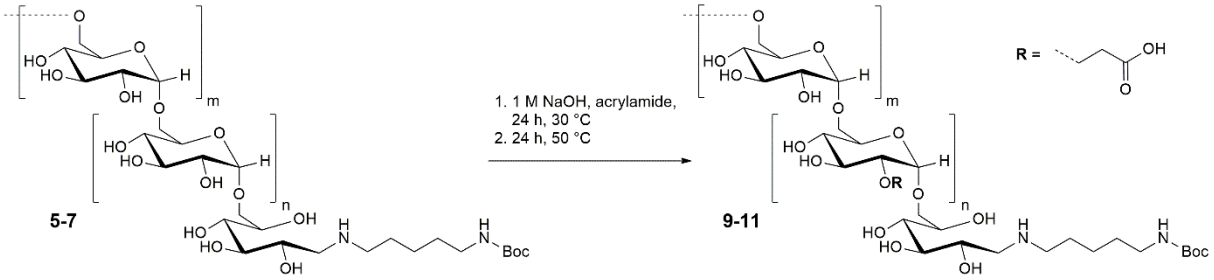

Scheme S 3. Carboxyethylation of Dex-*N*-Boc-Cad to 2-CED-*N*-Boc-Cad.

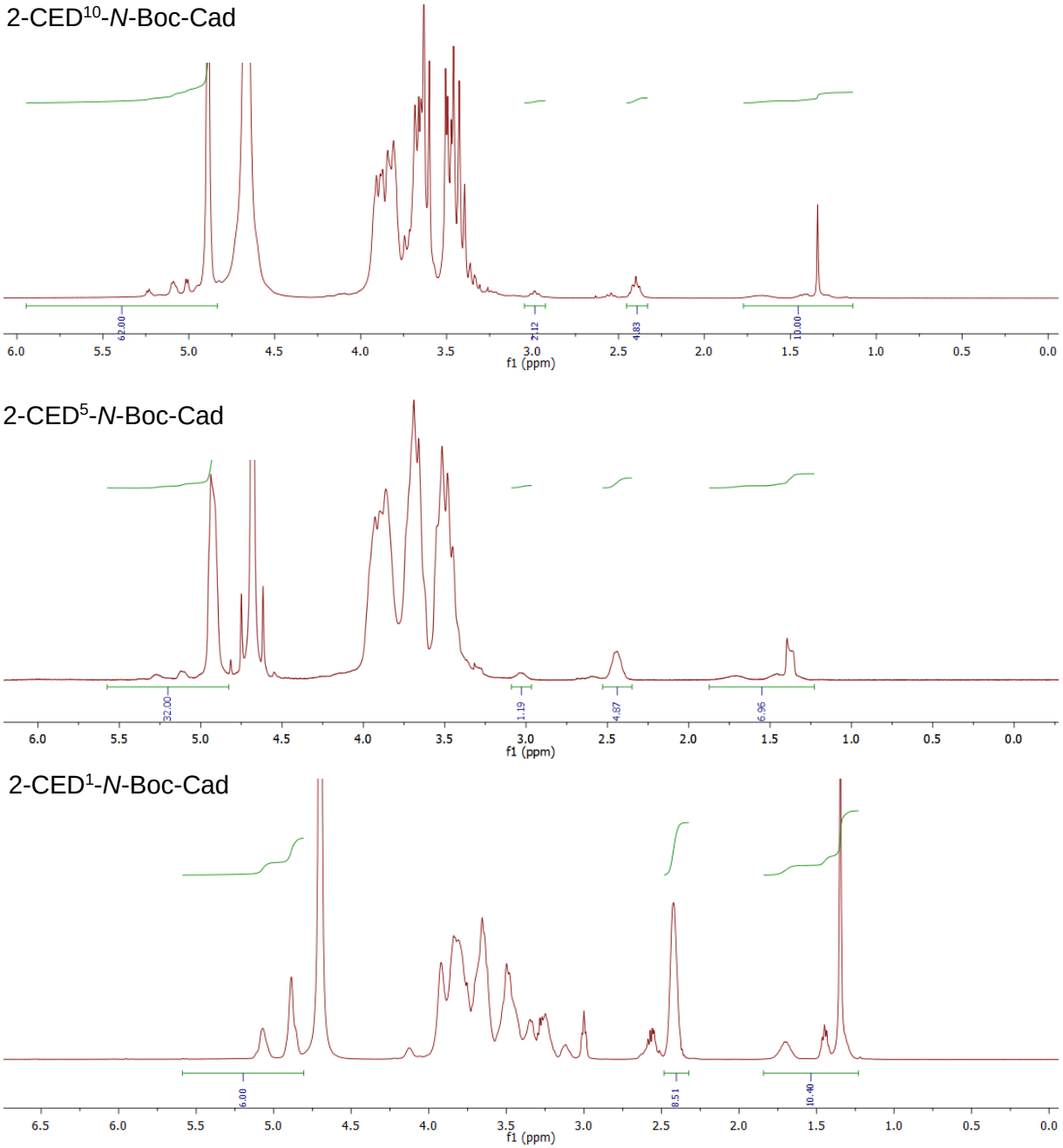

Figure S 4. ^{1}H-NMR spectra of 2-CED^{10}-*N*-Boc-Cad variants. ^{1}H-NMR of CE-dextranes (300 MHz, D_2O) δ = 6.09 – 4.79 (m, 1 H, C(1)H), 4.34 – 3.16 (m, C(2-6)H (glucose units); C**H**$_2$CH_2COOH), 3.14 – 2.91 (m, 4 H, C**H**$_2$NH-Boc, C**H**$_2$(CH_2)$_4$NH-Boc), 2.52 – 2.29 (t, C**H**$_2$COOH), 1.82 – 1.24 (overlapped m, 15 H, C**H**$_2$(CH_2)$_3$NH-Boc, C**H**$_2$(CH_2)$_2$NH-Boc, C**H**$_2$(CH_2)$_1$NH-Boc, 3 C**H**$_3$(Boc)) ppm.

1.4. Synthesis of N_3-dextran-*N*-Boc-cadaverine

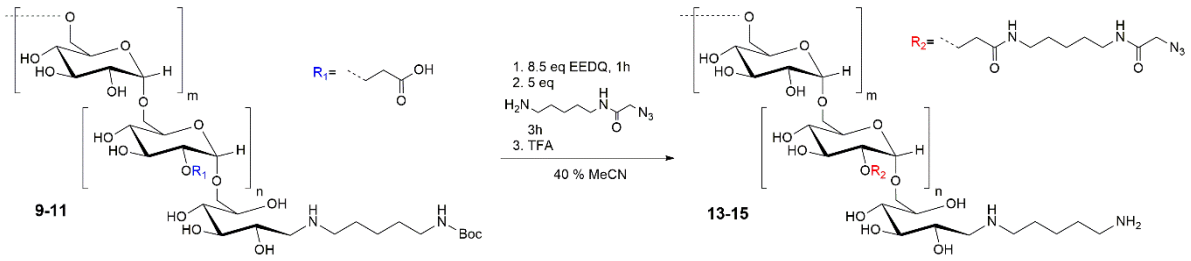

Scheme S 4. N_3-functionalization of 2-CED-*N*-Boc-Cad towards N_3-Dex-Cad.

Table S 2. Yields of N_3-functionalization of 2-CED-*N*-Boc-Cad with the N_3-cad-linker and determined number of N_3-groups per dextran (by ^{1}H-NMR).

compound	N_3-groups per dextran	Yield [%]
N_3-Dex^{10}-Cad	2.4	70
N_3-Dex^{5}-Cad	2.4	65
N_3-Dex^{1}-Cad	4.3	40

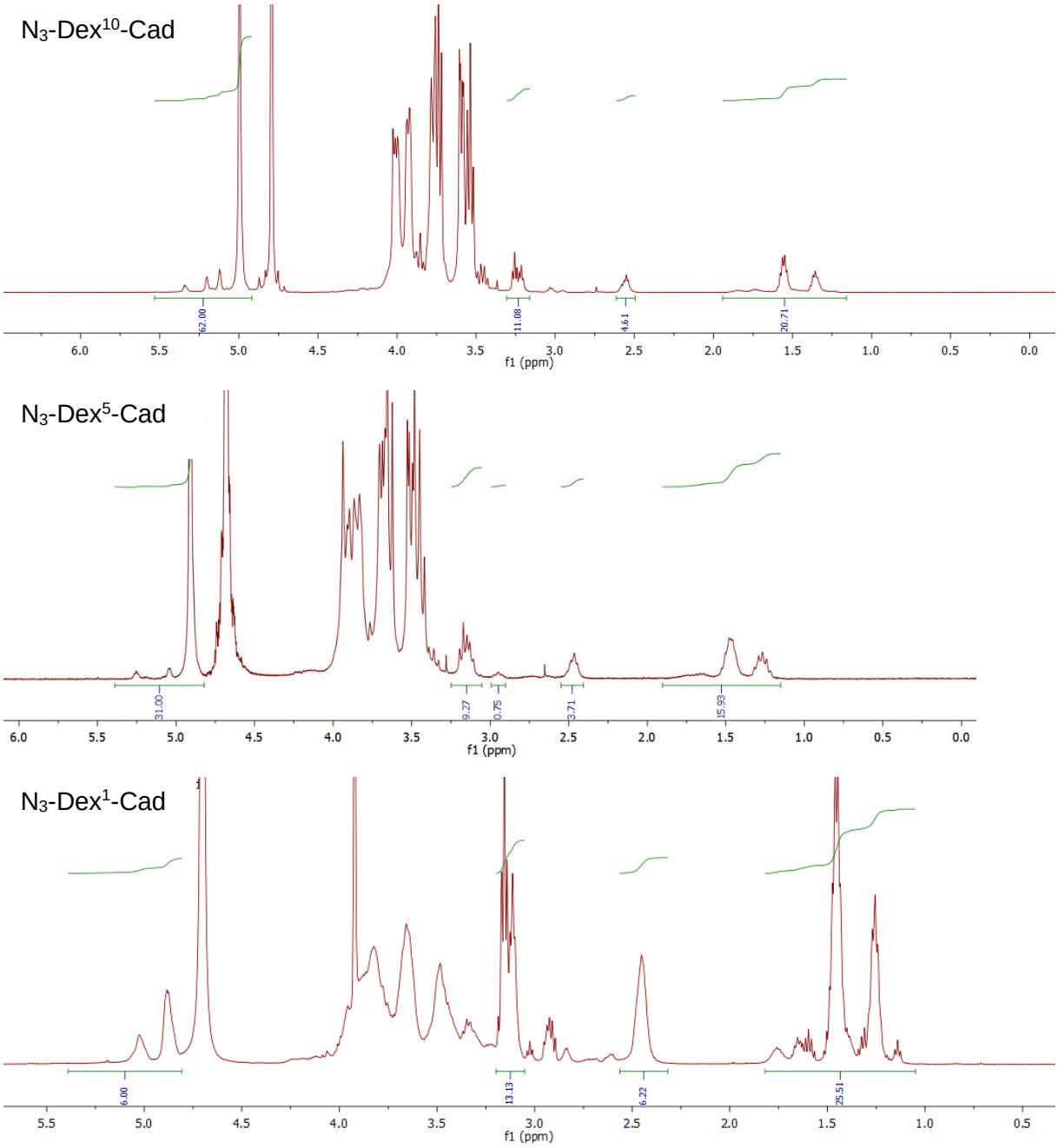

Figure S 5. ^{1}H-NMR spectra of N_3-Dex-Cad variants. ^{1}H-NMR (300 MHz, D_2O) δ = 6.24 – 4.80 (m, 1 H, C(1)H), 4.23 – 3.25 (m, C(2-6)H (glucose units); CH_2CH_2COOH; CH_2-N_3), 3.23 – 3.07 (m, NHCO-CH_2-N_3; CH_2-$(CH_2)_4$-NHCO-CH_2-N_3), 3.07 – 2.96 (m, 4 H, CH_2NH-BOC, $CH_2(CH_2)_4$NH-Boc), 2.73 – 2.34 (m, C**H**$_2$COOH), 1.80 – 1.19 (overlapped m, 15 H, C**H**$_2(CH_2)_3$NH-Boc, C**H**$_2(CH_2)_2$NH-Boc, C**H**$_2(CH_2)_1$NH-Boc, 3 C**H**$_3$(BOC); (1.80 – 1.37 C**H**$_2$-CH_2-NHCO-CH_2-N_3, C**H**$_2$-$(CH_2)_3$-NHCO-CH_2-N_3), 1.31 – 1.03 C**H**$_2$-$(CH_2)_2$-NHCO-CH_2-N_3)) ppm.

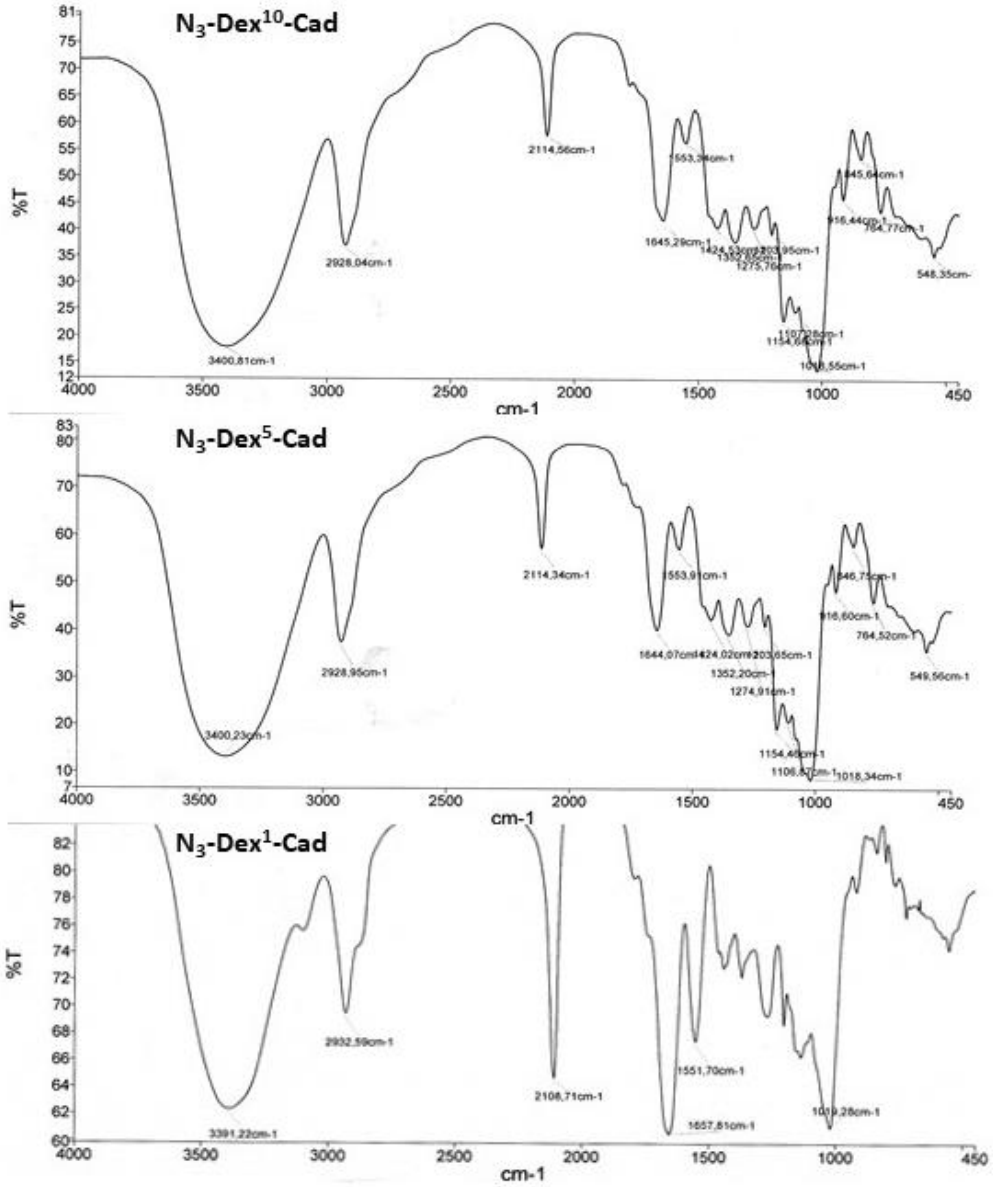

Figure S 6. IR-Spectra of N_3-Dex^{10}-Cad variants. N_3-stretching vibrational band: 2110 – 2115 cm^{-13}.

1.5. Synthesis of BCN-IRDye700DX

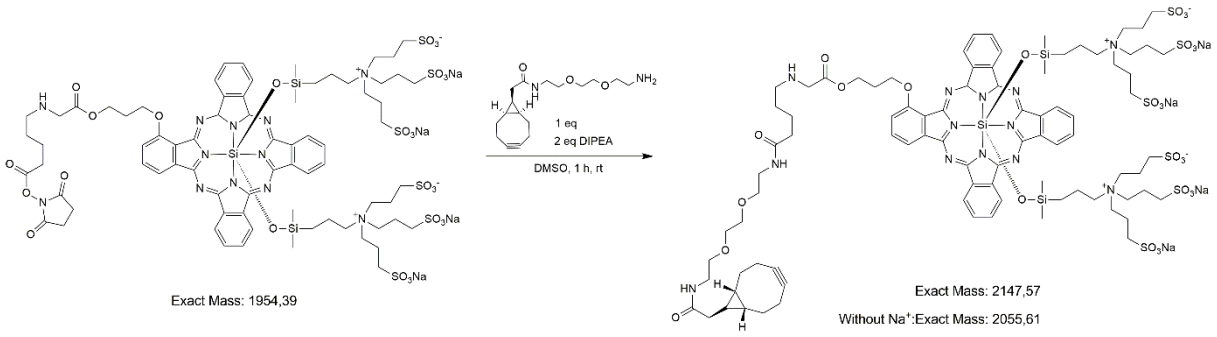

Scheme S 5 Synthesis of BCN-IRDye700DX.

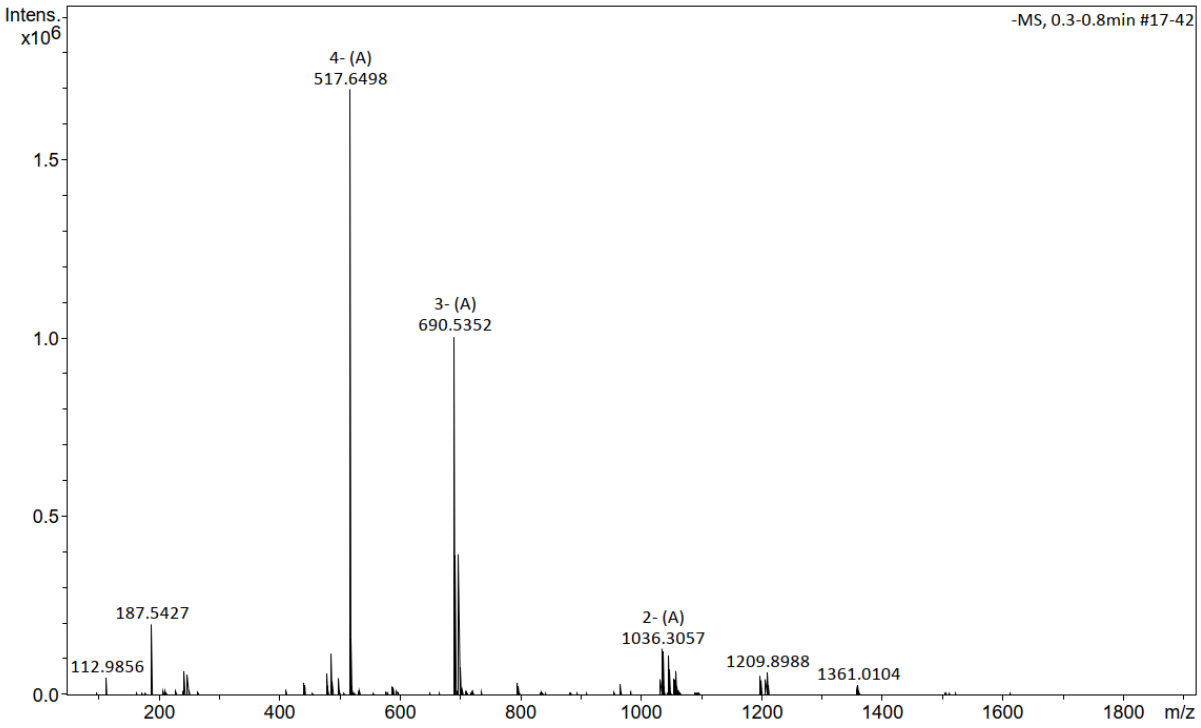

Figure S 7. ESI-MS spectrum of BCN-IRDye700DX®.

1.6. Structural formulas of utilized labels

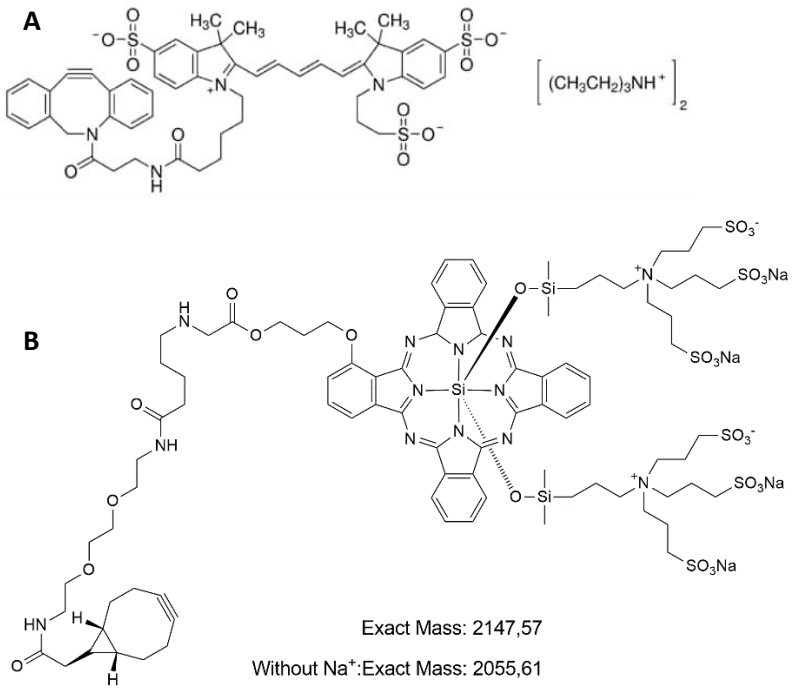

Scheme S 6. Utilized labels for SPAAC. **A**: DBCO-Cy5. **B**: BCN-IRsye700DX.

1.7. Generation of dextraknobs

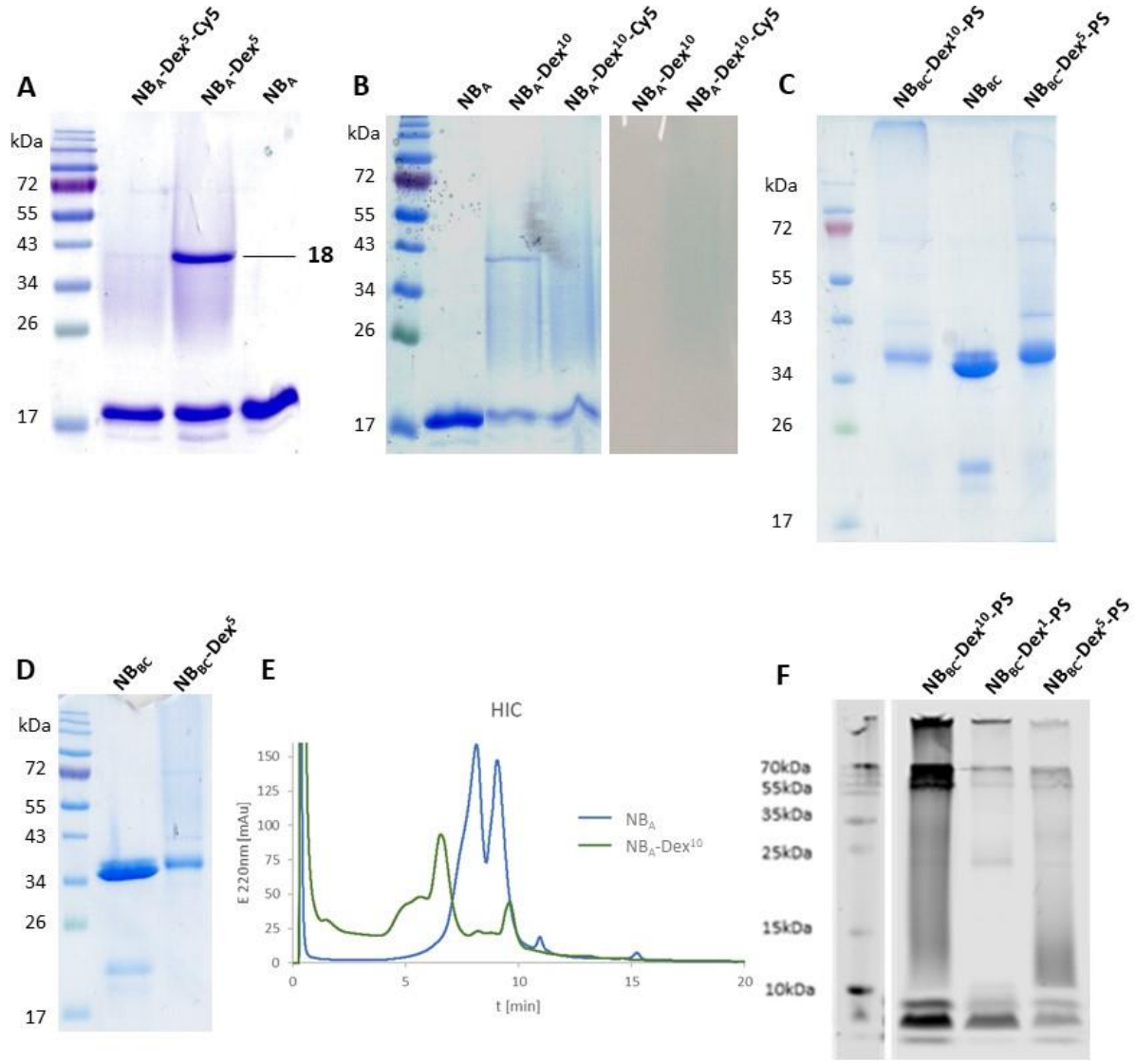

Figure S 8. A-D: Coomassie stained SDS-Gels of generated dextraknobs. **E**: HIC chromatogram of NB_A-Dex^{10}. **F**: SDS-Gel imaged with fluorescence reader (700 nm). Bands show excited IRDye700DX®.

2. Supplementary figures cell assays

2.1. Cellular binding assays

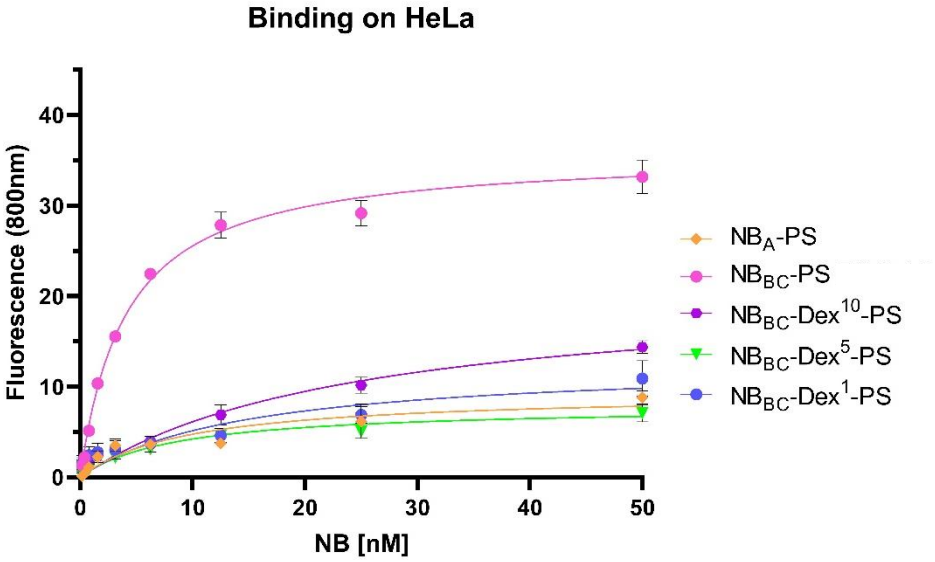

Figure S 9. Data of binding assay of NB-PS conjugates on HeLa cell line.

Table S 3. K_D-values of tested conjugates on HeLa cells.

	K_D HeLa [nM]
NB$_{BC}$-Dex^{10}-PS DOC 1.2	24.3
NB$_{BC}$-Dex^{5}-PS DOC 0.7	8.7
NB$_{BC}$-Dex^{1}-PS DOC 1.1	14.8
NB$_A$-PS-DOC 0.9	9.7
NB$_{BC}$-PS-DOC 1.5	4.1

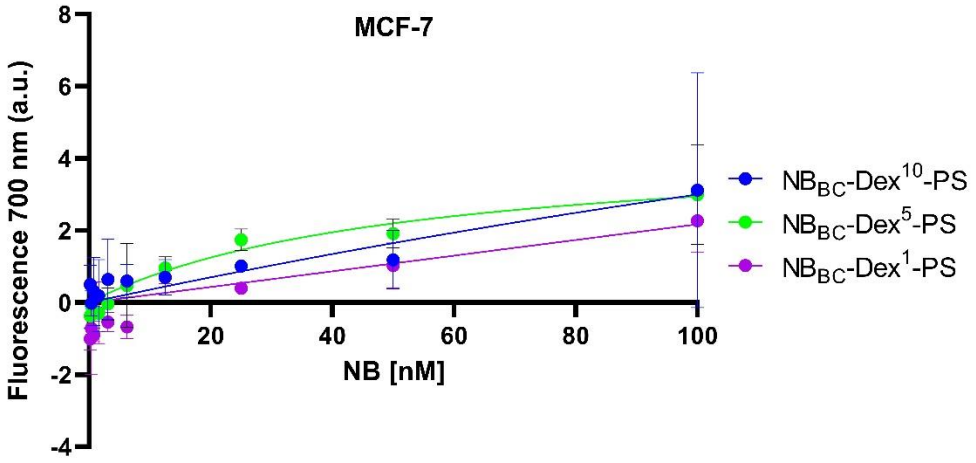

Figure S 10. Data of binding assay of NB$_{BC}$-Dex-PS conjugates on MCF-7 cells.

2.2. Confocal microscopy of spheroids

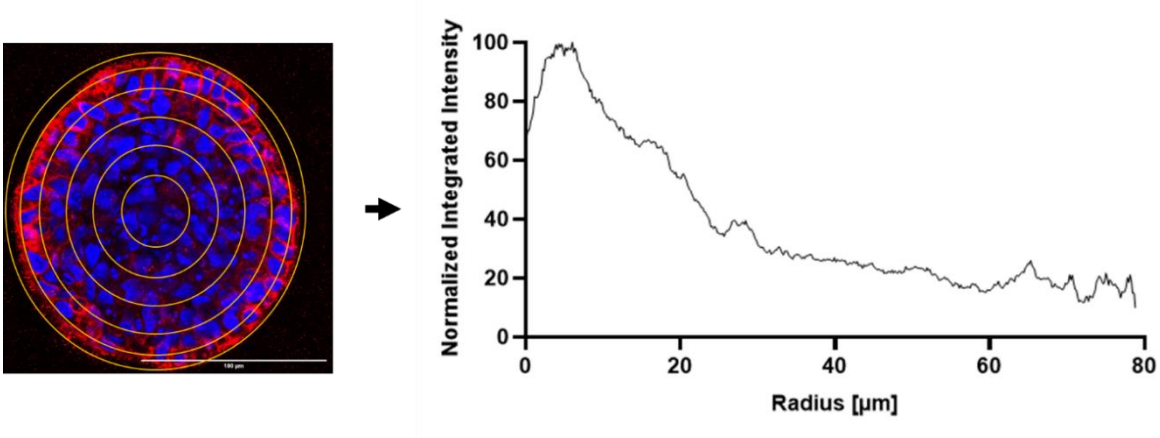

Figure S 11. Schematic representation of the analysis of confocal images taken of spheroids using ImageJ radial angle plug-in to create normalized integrated intensity plots of the NB signal along the radius of the spheroids.[7]

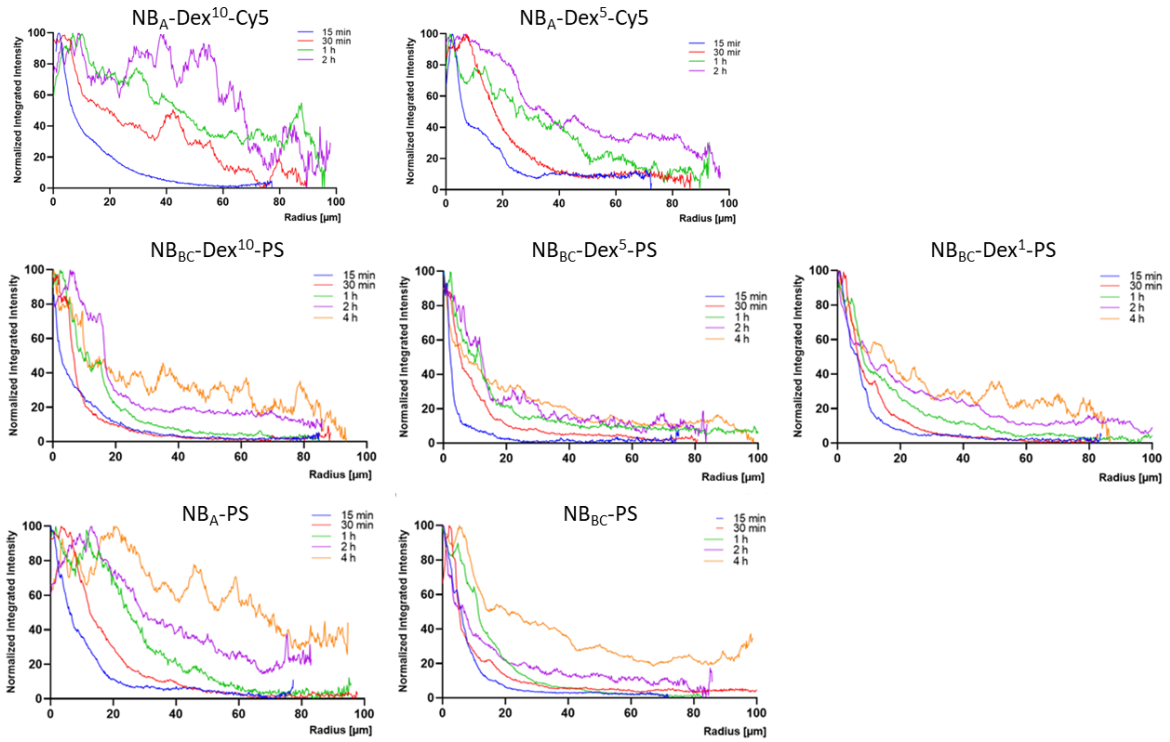

Figure S 12. Normalized integrated intensity plots of all conjugates at time points 15 min, 30 min, 1 h and 2 h. PS-conjugates were also measured at 4 h.

2.3. Nanobody-targeted photodynamic therapy (in vitro) on 2D monolayer cell culture

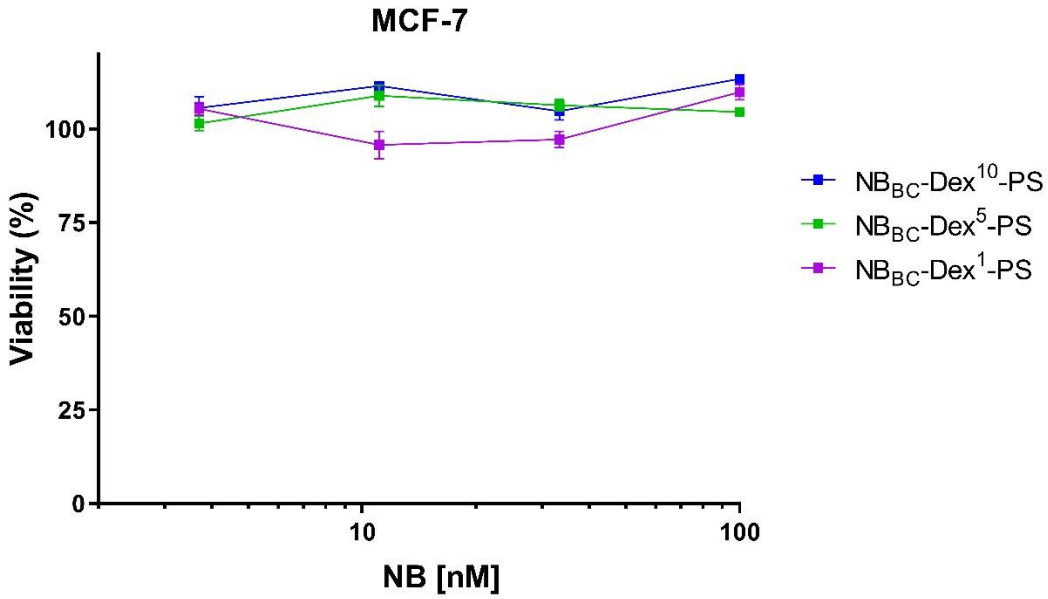

Figure S 13. Percentages (%) of cell viability after a 10 J/cm^2 light dose relative to untreated cells.

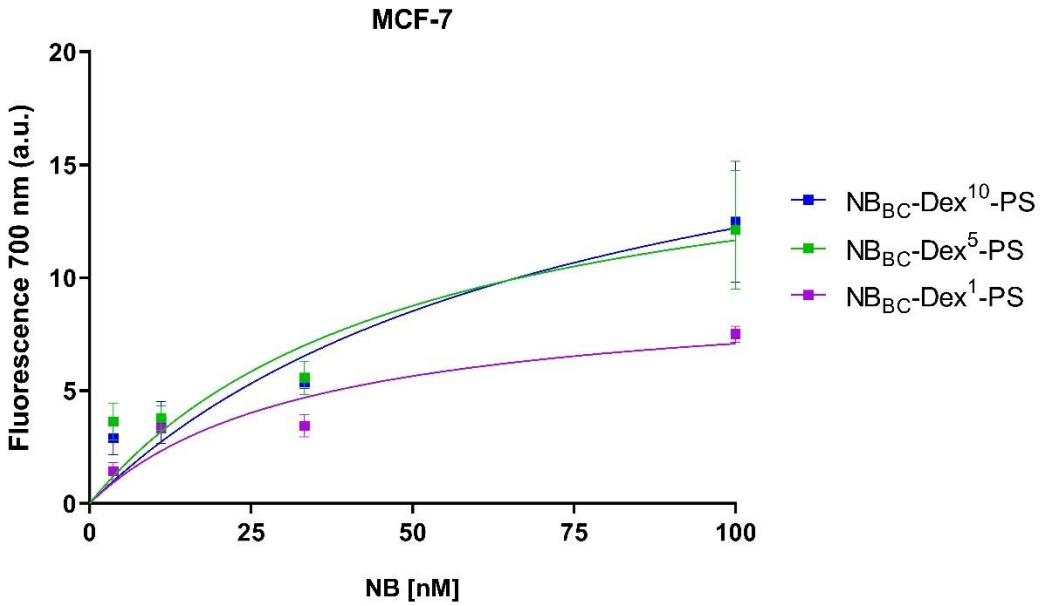

Figure S 14. Fluorescence intensities of NBBC-Dex--PS conjugates bound to cells after 30 min pulse incubation with a concentration range of the conjugates.

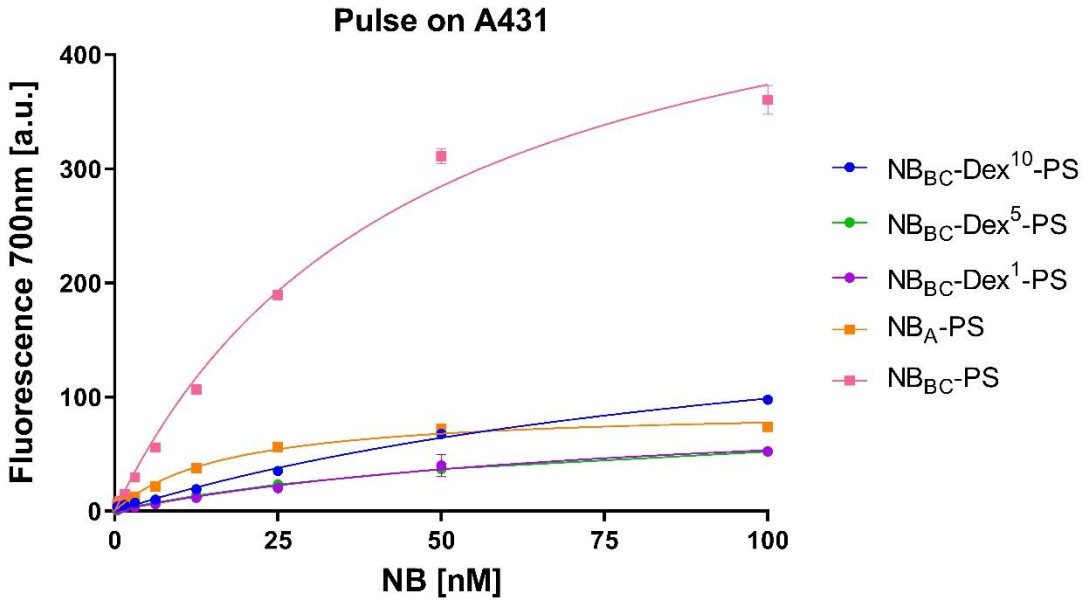

Figure S 15. Fluorescence intensities of NB-PS conjugates bound to cells after 30 min pulse incubation with a concentration range of the conjugates.

2.4. NB-targeted PDT on 3D spheroid cell culture

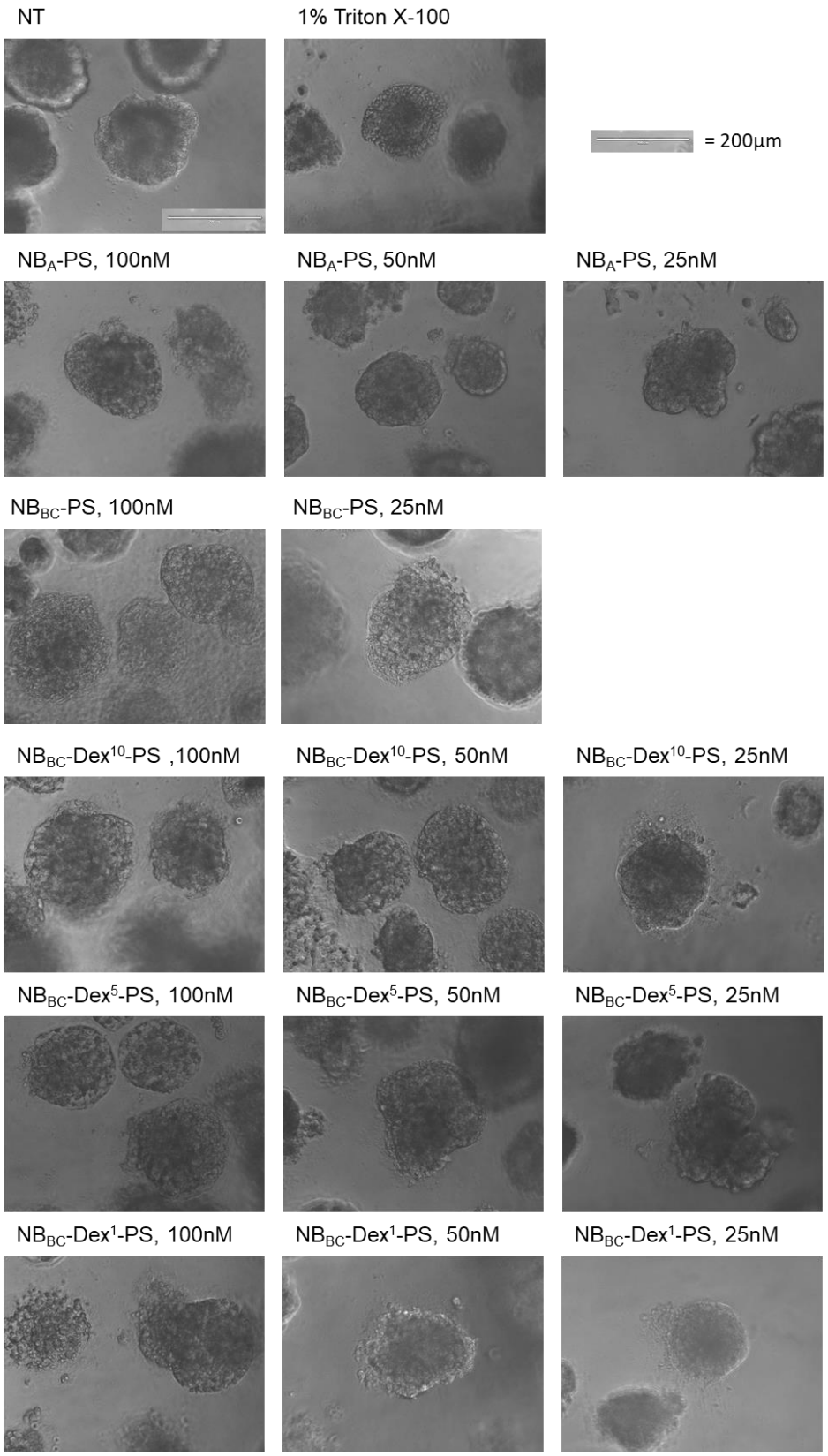

Figure S 16. 3D PDT 20J/cm^2, phase-contrast microscopy images taken 24h post treatment/irradiation.